Title
WATER TUNNEL WITH MOVING WALLS

Author
Atkins, Thomas.

Publication Date
1965-06-01

Thesis/dissertation

University of California

Ernest O. Lawrence Radiation Laboratory

WATER TUNNEL WITH MOVING WALLS

Berkeley, California

DISCLAIMER

Research and Development

UCRL-16188

UNIVERSITY OF CALIFORNIA

Lawrence Radiation Laboratory
Berkeley, California

AEC Contract No. W-7405-eng-48

WATER TUNNEL WITH MOVING WALLS

Thomas Atkins

(Master's Thesis)

June 1965

WATER TUNNEL WITH MOVING WALLS

Contents

WATER TUNNEL WITH MOVING WALLS

Thomas Atkins

Inorganic Materials Research Division, Lawrence Radiation Laboratory,
and Department of Chemical Engineering,
University of California, Berkeley, California

June 1965

ABSTRACT

The design of a recirculating water tunnel is described. The tunnel has a square cross-section, six inches on a side. It makes use of a system of moving walls as a calming section to allow the damping out of velocity fluctuations without permitting a boundary layer growth. The moving wall system is described in detail. The tunnel is designed to obtain turbulence levels as low as .0008% at Reynolds numbers up to 10,000 with a flat velocity profile.

A technique to allow photographic study of the flow using tellurium electrodes is outlined. These electrodes emit a black collidal suspension of tellurium which is very suitable for photographing.

A typical experiment to be performed in the tunnel is also described. It is the flow past a rectangular cutout, or notch, resulting in the formation of a stable eddy. In particular, the experiment would attempt to confirm the existance of secondary eddies in the corners of the notch.

INTRODUCTION

Within the field of fluid mechanics, the study of steady-state vortices is important and interesting. The desire to study the formation and structure of steady-state vortices provided the motivation for the construction of the water-tunnel described herein. It was desired that a flow-tunnel be developed, using water as the working fluid, which could provide laminar, or very low turbulence, flow at Reynolds numbers up to about ten thousand and, in addition, an approximately flat velocity profile.

The standard procedure used in wind tunnels to provide low turbulence, high Reynolds number flow is to pass the fluid through a series of screens or honeycombs, used as a flow-straightener, and then to contract the fluid to diminish the intensity of turbulence. The procedure adopted in this tunnel involves passing the water through a honeycomb flow straightener into a section of the tunnel in which the walls translate with precisely the bulk average water velocity. If the water were left in such a section for a long enough time, the disturbances created by the flow-straightener could be damped out to any desired degree. The effective Reynolds number in this section of the tunnel, which will be referred to as the moving-wall section, would be zero. It would further allow the establishment of a nearly flat velocity profile. Experiments could then be performed either within the moving-wall section itself or in a test-section immediately downstream. It was felt that this rather unusual technique would enable the production of very low-turbulence flow with little boundary-layer effects.

The design and construction of a recirculating water tunnel using the moving-wall technique is described in Sec. A of this work. It includes 1) the design of the moving walls, including theoretical considerations, 2) the remaining tunnel sections (the test section, flow-straightening section, and converging and diverging sections), and 3) the recycle system. Section B describes a technique for flow visualization, and a typical experiment to be performed in the tunnel is described in Sec. C.

A. DESIGN AND CONSTRUCTION

1. Moving Walls

a. Theoretical Considerations

Among the design considerations which can be examined from a theoretical point of view, the length of the moving-wall section is one of the most important. The water entering the moving-wall section will exhibit a velocity profile which will be relatively flat, but will have small "humps" or fluctuations corresponding to individual cells of the honeycomb used in the flow straightener. During passage through the moving-wall section of the tunnel, the effective Reynolds number of the flow will be zero, and these small spatial fluctuations in the velocity profile will tend to damp out due to natural viscous stresses. The moving-walls should therefore be long enough to allow these velocity fluctuations to damp out to some insignificantly small value.

In order to obtain some idea of what this length will be, the following simplified model is considered. The situation is represented in two dimensions as the steady, uniform, laminar flow past a series of finite parallel flat plates spaced evenly across a rectangular frictionless channel, as illustrated in Fig. A-1. It is then assumed that at some unknown (but, we hope, short) distance downstream of the plates, the velocity profile may be represented as the sum of the constant bulk average velocity, U, plus a small spatial fluctuation, u':

$$u = U + u' \qquad \text{(A.1-1)}$$

where u = local fluid velocity in the downstream (X) direction

U = bulk average velocity (a constant)

u' = a velocity fluctuation

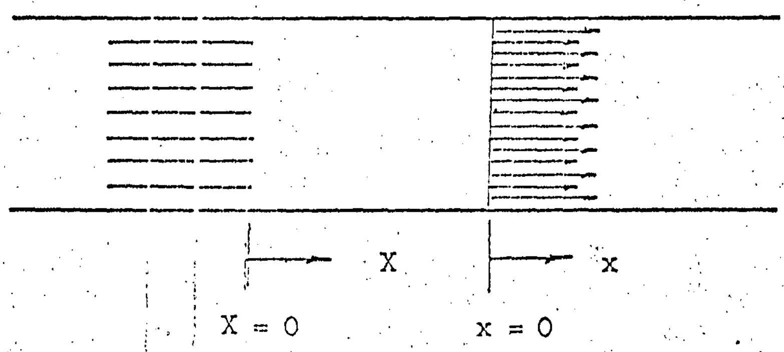

FIGURE A-1

and $$u' << U. \tag{A.1-2}$$

In particular, the boundary condition on the fluctuation u' is assumed for simplicity to be of the form:

$$u' = A \cos \frac{\pi y}{h} \tag{A.1-3}$$

where A = the amplitude of u' at x = 0

y = the cross-stream coordinate

and h = one-half the distance between plates.

This relation is illustrated in Fig. A-2. The local fluid velocity may now be written as:

$$u = U + A \cos \frac{\pi y}{h} \tag{A.1-4}$$

The following non-dimensional variables are introduced:

$$u^* = \frac{u}{U} \qquad v^* = \frac{v}{U} \qquad u'^* = \frac{u'}{U}$$

$$x^* = \frac{x}{2h} \qquad y^* = \frac{y}{2h} \tag{A.1-5}$$

so that the velocity u* becomes:

$$u^* = 1 + \frac{A}{U} \cos 2\pi y^* \tag{A.1-6}$$

or $$u^* = 1 + u'^*$$

where $$u'^* \ll 1 .$$

Inserting this expression for u* into the non-dimensional Navier-Stokes equations and neglecting terms of second order in u'*, as well as the streamwise pressure gradient, we are left with the following linear partial differential equation:

$$\frac{\partial u'^*}{\partial x^*} = \frac{1}{Re_h} \left(\frac{\partial^2 u'^*}{\partial x^{*2}} + \frac{\partial^2 u'^*}{\partial y^{*2}} \right) \tag{A.1-7}$$

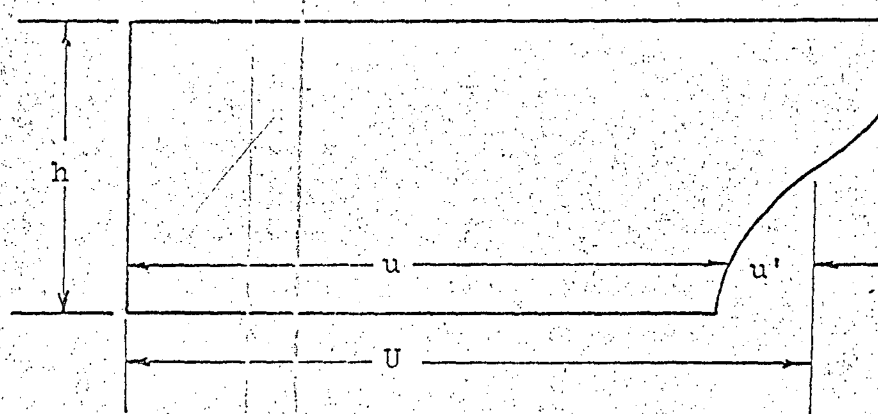

FIGURE A-2

where $$Re_h = \frac{2hU}{\eta}$$

and η = kinematic viscosity.

The boundary conditions to be applied are:

1) $$\text{at } x^* = 0,\ u'^* = \frac{A}{U} \cos 2\ y^* \qquad \text{(A.1-8)}$$

2) $$\frac{\partial u'^*}{\partial y^*} = 0 \text{ at } y^* = \frac{n}{2}\ (n = 0, 1, 2, 3, \ldots.) \qquad \text{(A.1-9)}$$

3) u'^* is finite or zero at $x = \infty$. (A.1-10)

The problem is solved in detail in Appendix A, the solution being:

$$u'^* = \frac{A}{U} \cos 2\pi y^* \cdot \exp(-rx^*) \qquad \text{(A.1-11)}$$

where $$r = -Re_h + \sqrt{Re_h^2 + 4\pi^2}\ .$$

The important result of this solution is r, for it determines the rate of damping. Notice that the exponent is always negative. For the case where $Re_h \gg 2\pi$ (which is in the region of interest), r may be approximated by:

$$r = \frac{2\pi^2}{Re_h} \qquad \text{(A.1-12)}$$

so that:

$$u'^* = \frac{A}{U}\ \cos(2\pi y^*)\ \exp\left[-\left(\frac{2\pi^2}{Re_h}\right) x^*\right] \qquad \text{(A.1-13)}$$

Two additional factors must be known before we can calculate the magnitude of u' at any distance downstream of the plates: 1) the distance X = L from the plates which corresponds to x = 0 in the above solution for u' (i.e., the distance L at which our initial assumption $u' \ll U$ becomes valid); and 2) the amplitude A at X = L (x = 0).

The rate of damping in the region $0 \leq X \leq L$ cannot be predicted from this analysis, but because of the steep velocity gradients, it is expected to be much faster than in the region $X > L$.

It is reasonable to assume that a conservative estimate of the length L and corresponding amplitude A may be found by considering the flow in the wake of a single finite flat plate. For this case, it is found that u* achieves a value of 0.8 at a distance X of about three plate lengths.[1] The plate length most appropriate for our purposes is the length ℓ required to obtain fully developed laminar flow in a two-dimensional channel made of flat parallel walls separated by a distance 2h. This may be given by[2]

$$\frac{\ell}{2h} = \frac{Re_h}{25}$$

so that

$$\frac{L}{2h} = \frac{3Re_h}{25} \tag{A.1-14}$$

Using this information as our initial condition (x = 0), the velocity u* becomes:

$$u^* = \frac{u}{U} = 1 + 0.2 \cos(2\pi y^*) \exp\left[-\left(\frac{2\pi^2}{Re_h}\right) x^*\right] \tag{A.1-15}$$

Figure A-3 is a plot of u/U versus X/2h for y* = 0. The Reynolds number of the tunnel, Re_t, based on a six inch square cross-section, is used for convenience in place of Re_h. Note that the point x = 0 is located from Eq. (A.1-14).

On the basis of this analysis, a moving-wall length of 12-inches and a honeycomb mesh size 2h of 1/16 inch were chosen. This corresponds to X/2h X/2h = 192. The magnitude of the disturbance u'/U is approximately 0.000008 at this point for the maximum expected tunnel Reynolds number of 15,000. This corresponds to a pseudo-turbulence level, 100 u'/U, of .0008%, which compares very favorably with low turbulence wind tunnels.[3]

The analysis described above is not meant to provide an exact or even a very accurate solution to the damping problem. The fundamental assumption made here is that the flow does not become turbulent throughout

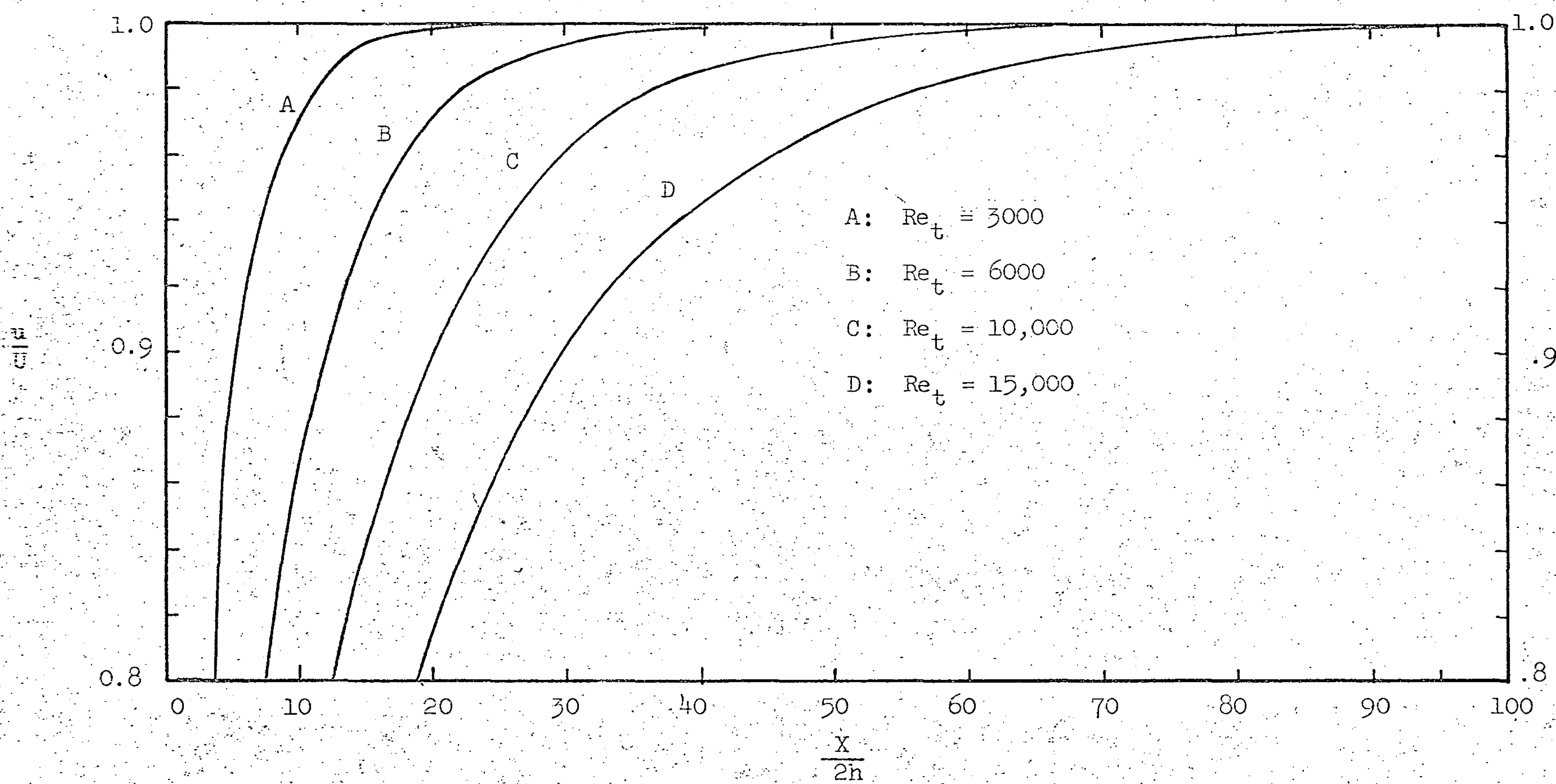

DAMPING OF VELOCITY FLUCTUATIONS

Fig. A-3

the damping period. The length of the honeycomb flow straightener can be simply adjusted so as to be sure that the flow within them will be laminar. The problem of turbulence exists in the wake of the honeycomb. G. I. Taylor[4] solved essentially the same problem under the assumption that the wake flow may be represented by homogeneous, isotropic turbulence. In this case, he obtained a solution for the velocity fluctuation u' proportional to the reciprocal of the downstream coordinate. Experimental evidence[5] indicates that for high Reynolds numbers this is a good assumption. Unfortunately, most of these data are taken in wind tunnels where the Reynolds numbers are a factor of ten or more higher than those which are of interest here.

Batchelor[5] discusses the existence of two periods in the decay of turbulence behind a grid. His first period is characterized by a complete dominance of the inertial terms in the Navier-Stokes equation. This is equivalent to Taylor's assumption and results in the same solution. According to Batchelor, however, the diffusion terms of the Navier-Stokes equation become more and more important downstream of the grid, until the final period is encountered where the diffusion term is dominant. The damping in this period would be characterized by an exponential solution such as described here. As Batchelor indicates, the final period is encountered closer and closer to the grid as the grid Reynolds number is reduced. This provides some indication that at the comparatively low Reynolds numbers of interest here, an exponential solution is likely. Until the tunnel can be tested under operation conditions, however, the question of the existence of turbulence in the wake of the flow straightener will not be resolved.

The approximate length of moving-walls required to deliver a flat, uniform, laminar velocity profile to the test section has been calculated. We should now like to see how rapidly the boundary layer will grow in the test section.

In order to calculate the boundary layer profile, we use the approximate relation for the laminar boundary-layer thickness on a long flat plate:

$$\frac{\delta}{X} = \frac{5}{\sqrt{Re_x}} \qquad (A.1\text{-}16)$$

where δ = boundary layer thickness

X = length downstream of the leading edge

or for convenience:

$$\frac{\delta}{D} = \frac{5}{\sqrt{Re_{tunnel}}} \sqrt{\frac{X}{D}} \qquad (A.1\text{-}17)$$

where: D = tunnel diameter

$$Re_{tunnel} = \frac{DU}{\eta}$$

The boundary layer profiles are plotted in Fig. A-4 using a tunnel diameter D of 6 inches.

We may anticipate here that in attaching the moving-wall section to the test section, a short length immediately downstream of the end of the moving walls will be unavailable for experimenting. These boundary layer profiles emphasize the need to keep this distance as short as possible to allow a small boundary layer thickness entering the test section.

Transition of the laminar boundary layer to a turbulent one will occur at a point downstream given approximately by

$$Re_x \approx 300{,}000 \qquad (A.1\text{-}18)$$

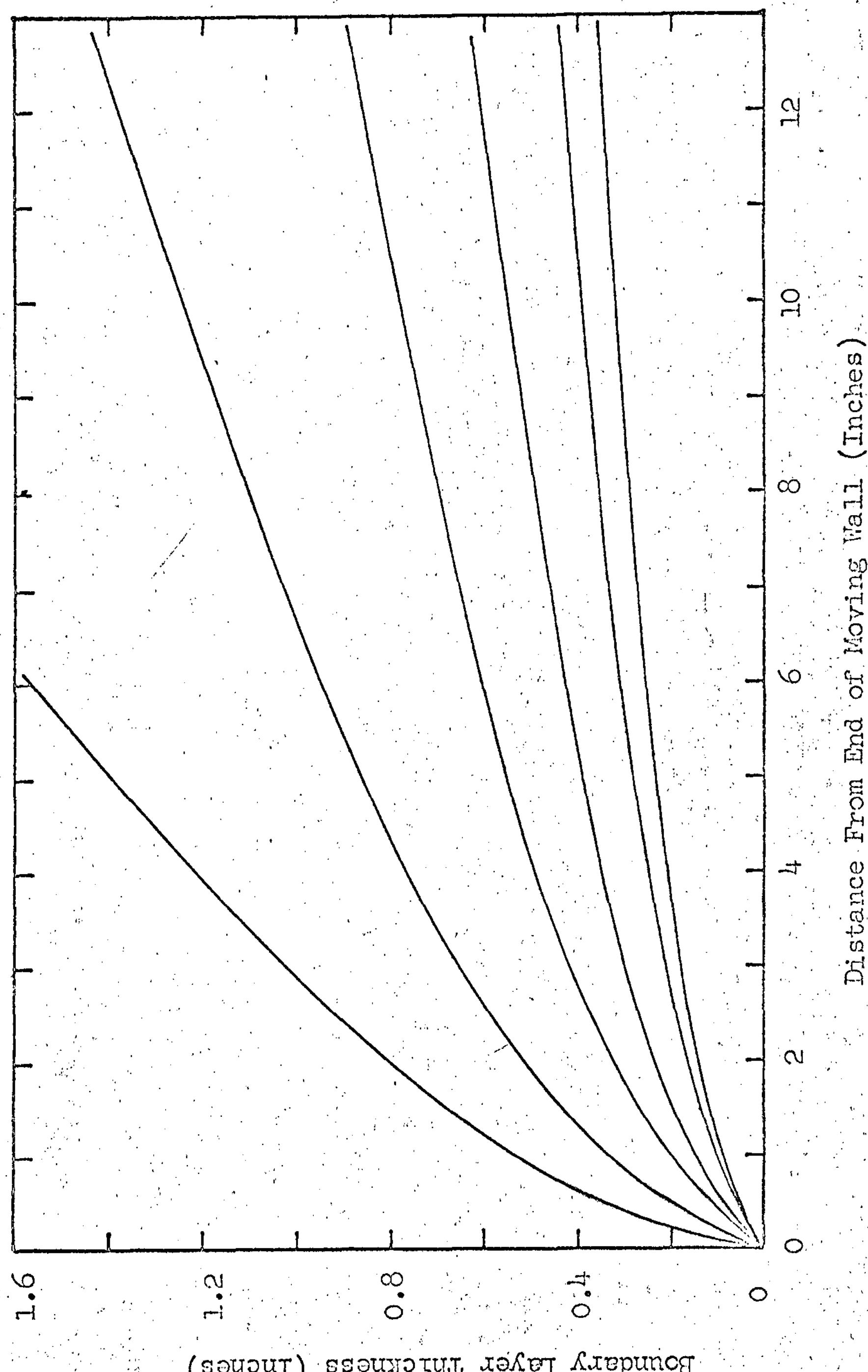

1.6
1.2
0.8
0.4
0
Boundary Layer Thickness (Inches)
0
2
4
6
8
10
12
Distance From End of Moving Wall (Inches)

FIGURE A-4

where Re_x is defined as before or

$$Re_t \approx 300,000 \left(\frac{D}{X}\right)$$

where Re_t is again based on the tunnel diameter D. Hence

$$X \approx 3\times10^5 \left(\frac{D}{Re_t}\right) \qquad (A.1-19)$$

The highest tunnel Reynolds number expected is approximately 15,000 so that the shortest length X required to produce a turbulent boundary layer is approximately

$$X = 3\left(\frac{6}{15,000}\right) 10^5 = 100 \text{ inches.}$$

Since the test section will be about 10 inches long, the boundary layer is expected to remain laminar.

b. Moving Wall System Design

In this section, the design and construction of the moving wall apparatus is described in detail. The section is subdivided into four parts, corresponding to the four most prominent design criteria: 1) the leakage problem, 2) the overall configuration, 3) the drive system, and 4) the belts.

So far only a general idea has been developed here of what the system will look like. It must consist of four continuous belts, one for each wall of the tunnel, whose width must be nearly equal to the width of a tunnel wall. In addition, each belt must enter the tunnel at the upstream end of the section and leave the tunnel at the downstream end. This will have to be accomplished through some kind of slots in the tunnel walls.

The first, most obvious problem which arises here is one of leakage. These slots promise to be a serious trouble spot. There exist two alternatives: one is to do our best in sealing these slots while leaving relatively free passage for the belts. This is obviously a very doubtful procedure as we are sure the leaks can never be completely eliminated.

It was therefore decided to proceed with the second alternative: to enclose the entire tunnel and belt arrangement in a housing which would extend over the whole length of the moving-wall section. This is illustrated in Fig. A-5. The housing itself could then be filled with water and leakage would be prevented. The design of this housing should be relatively independent of the belt system inside it, but is governed by one main principle: it must completely come apart for ease of inspection, assembly and repair of the belt system. It was considered sufficient to have the four outer surfaces of the housing removable. Lucite (or plexiglas) was chosen as the material for construction due to its ease in fabrication, transparency, and light weight.

The upstream end of the housing presents little problem. It can simply be flanged to the preceding (flow-straightening) section. At the downstream end, however, we wish to have the belt leave the tunnel as closely as possible to the entrance of the test section. It was therefore decided to join the moving-wall housing to the test section by a butt-joint, sealed with a single large O-Ring.

<u>Overall system configuration</u>. We now envision the system as consisting of four continuous belts, each entering a tunnel wall upstream and leaving that wall downstream. In addition, the belts must be driven by some system of rollers.

This leaves several choices for the design of the unit. The section of tunnel enclosed inside the housing may consist of 1) a single piece of sheet steel, folded and welded into a square cross-section, or 2) four

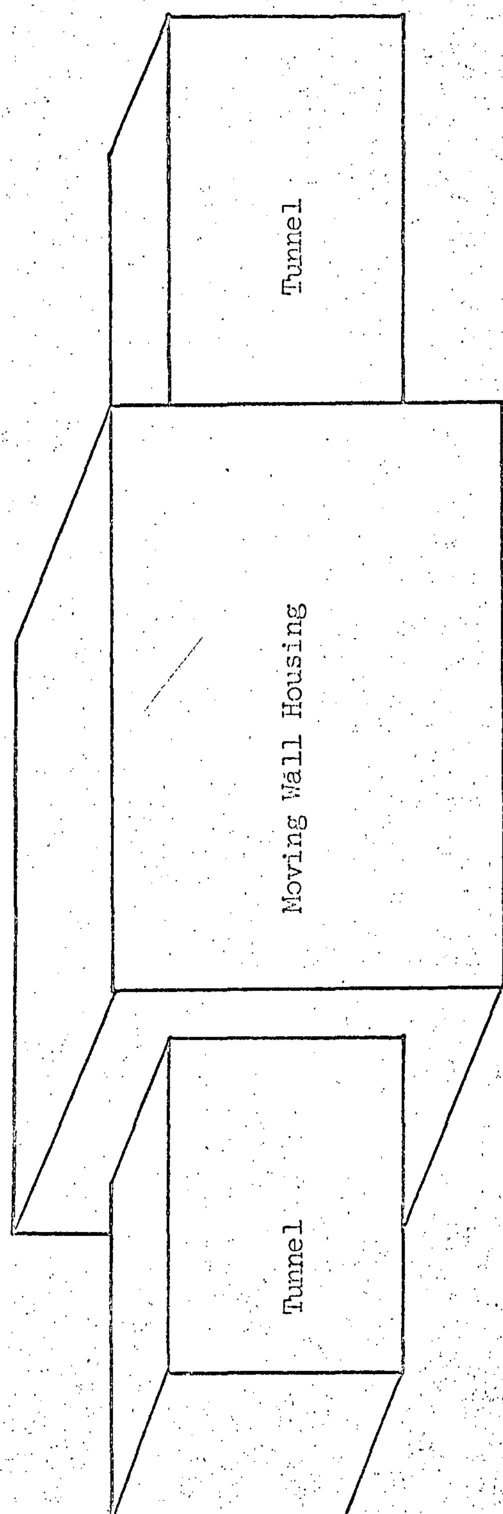

FIGURE A-5

separate walls not connected to each other, but to some part of the housing. In addition, the rollers may be mounted on either a) the tunnel walls, b) the fixed ends of the housing, or c) the removable sides of the housing. This allows six possible configurations to choose from: 1a, 1b, 1c, 2a, 2b, and 2c. Choice number 1 of the tunnel design would require that this section of tunnel be connected to the upstream and downstream sections at the corners only to allow slots for the belts, or that the slots be cut into this section of tunnel as closely as possible to the corners, again leaving attachment at the corners only. This presents a serious structural problem. In addition, it means that to change a belt, a strip of belt material must be threaded into the upstream slot, out of the downstream slot, and spliced into place, all while on the equipment (obviously not an easy task). Choice 2, however, permits complete removal of the tunnel wall with the housing face. This is very appealing, since it permits construction of the whole moving-wall section in five separate and independent units, namely the housing framework and four identical wall-units. Each wall unit would consist of a tunnel wall, a housing face, and the complete system of belt and rollers. This is the configuration finally chosen. It represents what I consider to be the most flexible design, permitting the maximum ease of fabrication, inspection, maintenance and repair. Figure A-6 illustrates the general configuration, omitting the roller system, which will be explained in the following section.

c. Drive System

The first, most basic requirement of the drive system is that all four moving walls be driven at precisely the same speed. Based on the overall configuration described in the preceding section, it was decided to drive each belt with a single roller, with each of these four rollers

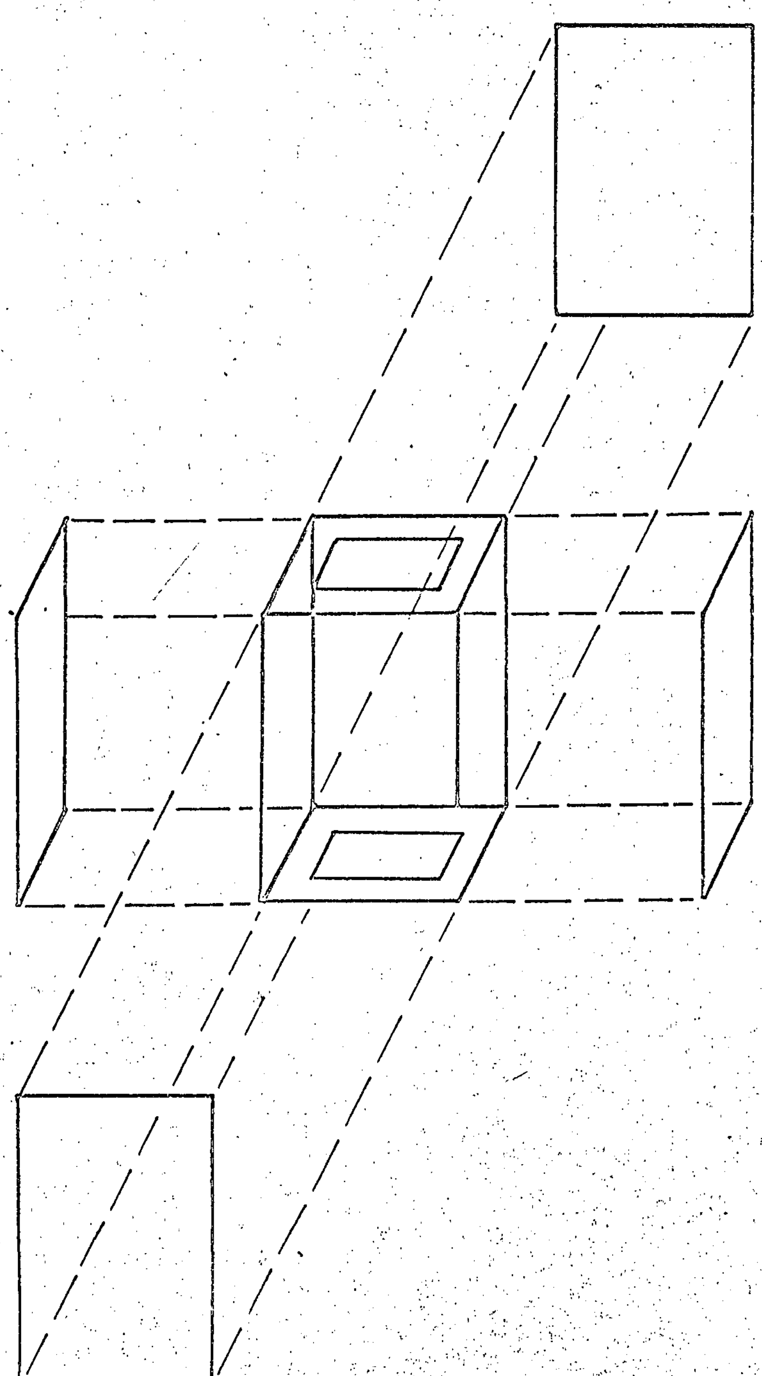

Moving Wall Housing

FIGURE A-6

geared at the corners and all four rollers driven by a single drive shaft (see illustration, Fig. A-7). The drive rollers were placed at the downstream end of each wall unit. Correspondingly, a "free" roller was placed at the upstream end of each unit. In addition, there must be some way to adjust the tension in each belt. Tension adjustment is required in order to 1) allow installation of belts while loose, 2) prevent slippage of the drive roller, 3) compensate for irregularities inevitable in splicing the belts, and 4) maintain control over the tendency of the belts to "drift" on the rollers. The last item was found in tests to be a far more severe problem than was anticipated and will be explained further in the next section. The method selected for tension adjustment is illustrated in Fig. A-8. This method provides independent, external adjustment on each side of the tension rollers. It has been found in tests to be adequate in setting up and maintaining good operation.

The final roller design is given in Fig. A-9. In addition to the above, this design was chosen to conserve space, permit maximum wrap-around on the drive roller, and ease of disassembly wherever possible.

All bearings used for the rollers are of a nylon-sleeve type. Testing of the completed units indicates that these bearings are sufficient. If, however, frictional problems arise with further testing, ball bearings may be installed without serious difficulty.

Care was taken in the corners to overcome the obvious space problem where adjacent wall-units meet. A difficult aspect of the construction occurred in matching all four walls in the corners, while maintaining the six inch square tunnel cross section and good matching with the upstream and downstream sections. Furthermore, these tolerances must be reproducible after disassembling and reassembling many times. A considerable effort was

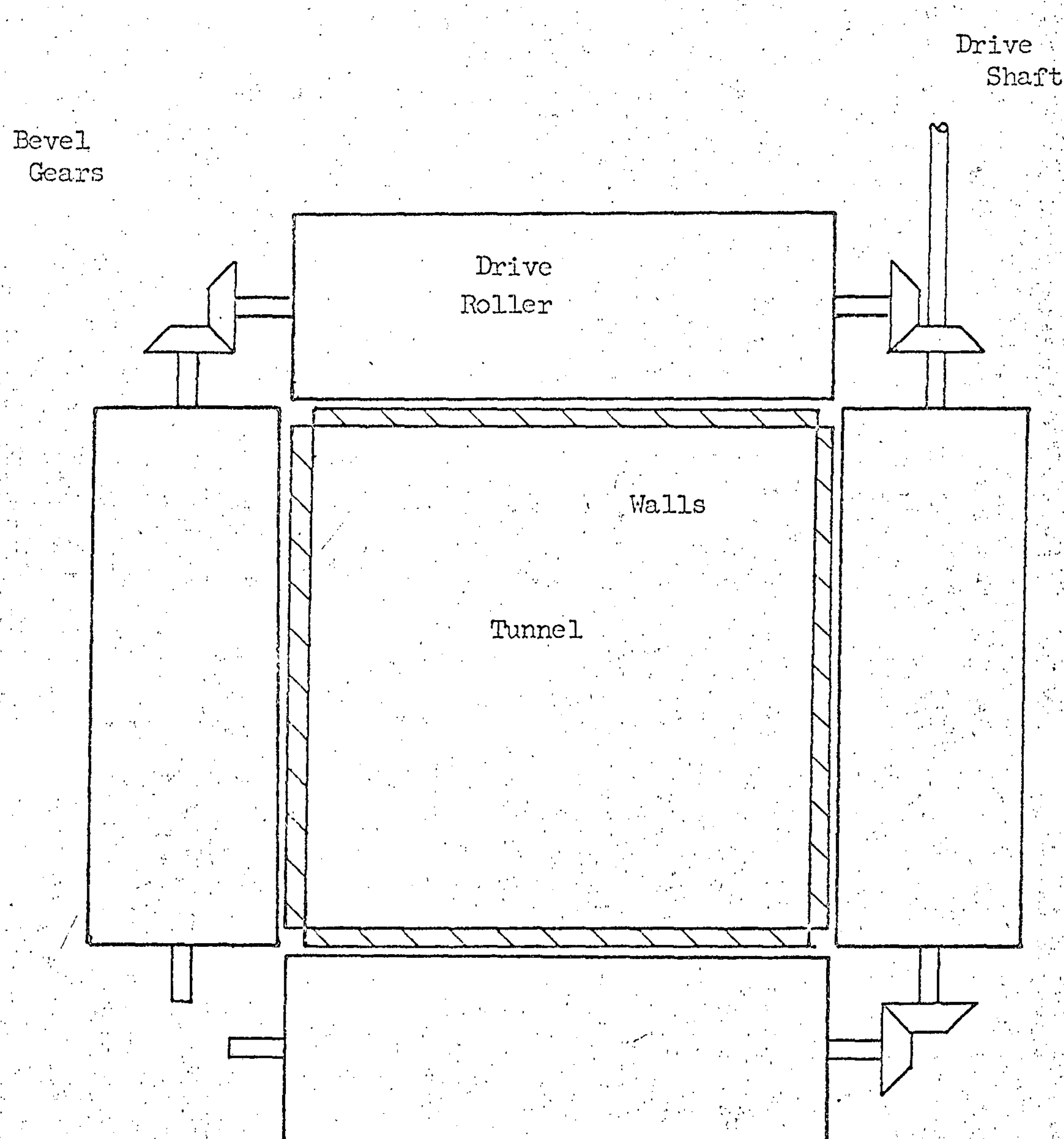

FIGURE A-7

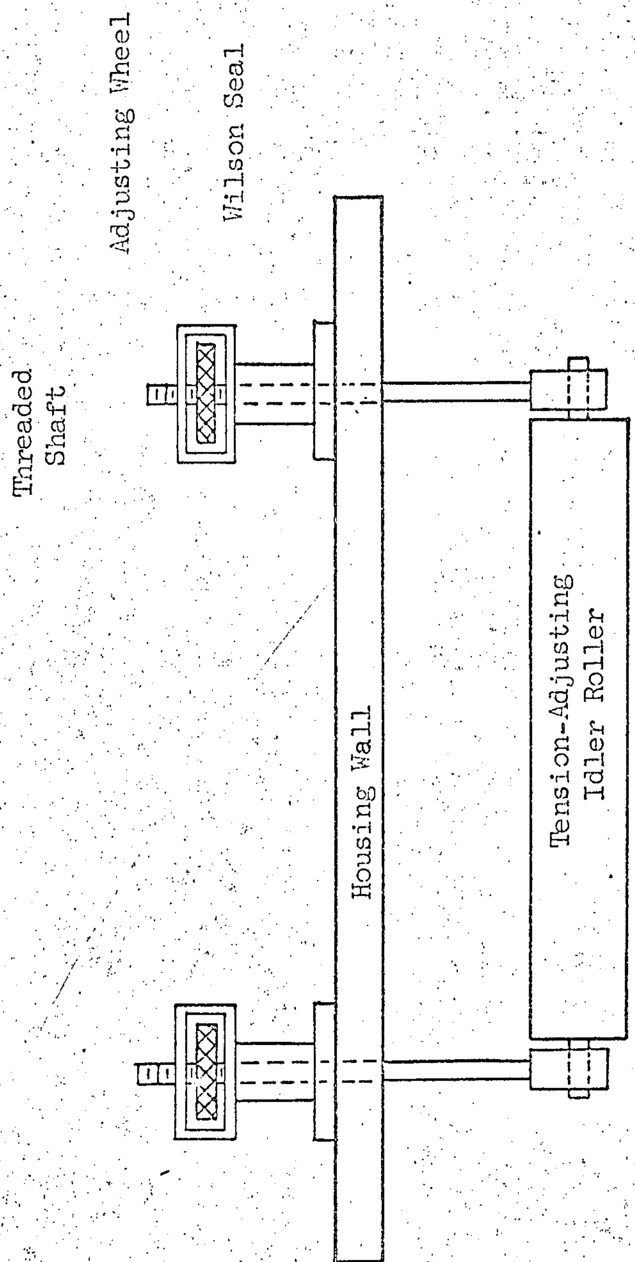
Threaded Shaft
Adjusting Wheel
Wilson Seal
Housing Wall
Tension-Adjusting Idler Roller

FIGURE A-8

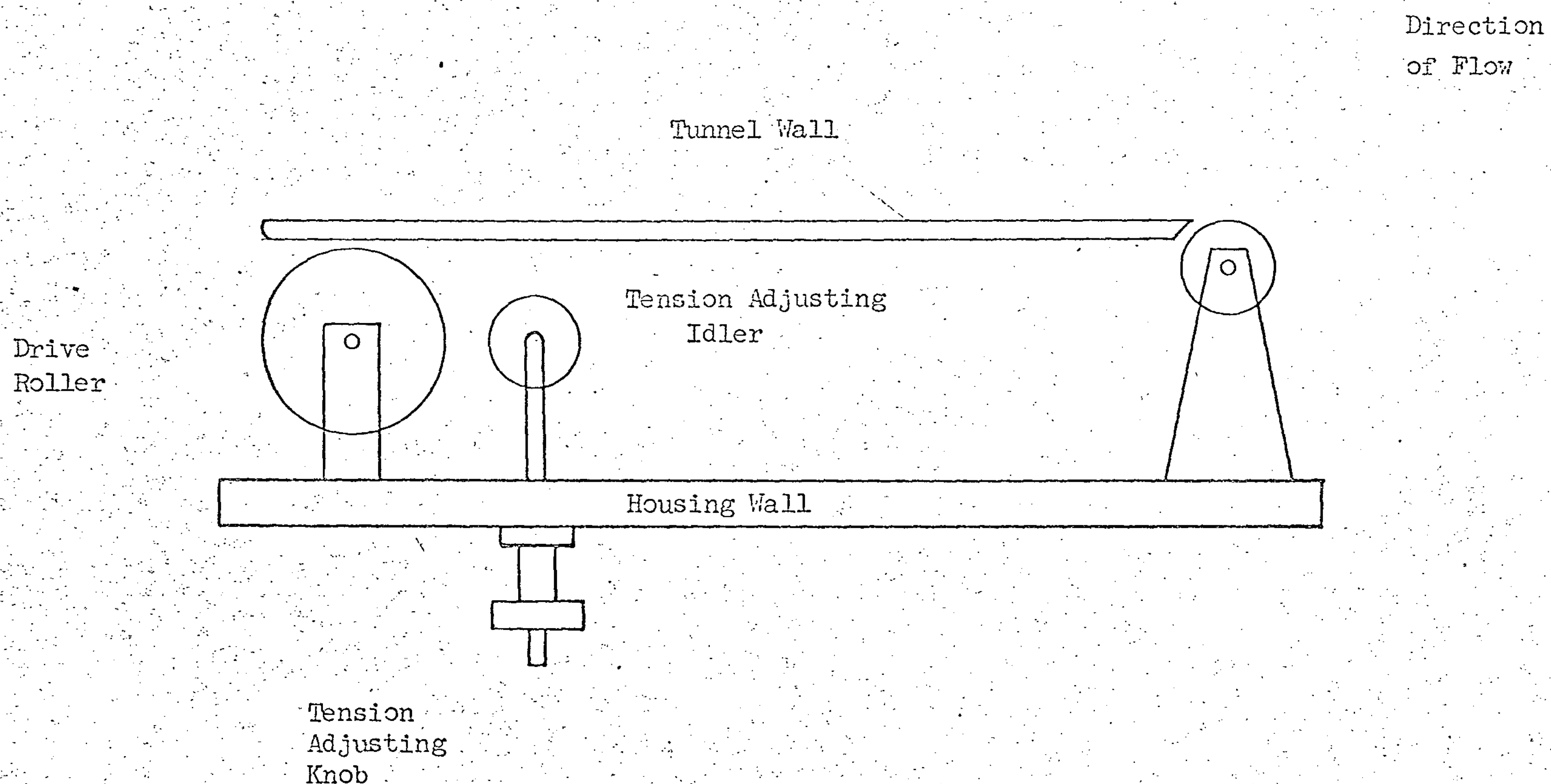
Direction
of Flow
Tunnel Wall
Tension Adjusting
Idler
Drive
Roller
Housing Wall
Tension
Adjusting
Knob

FIGURE A-9

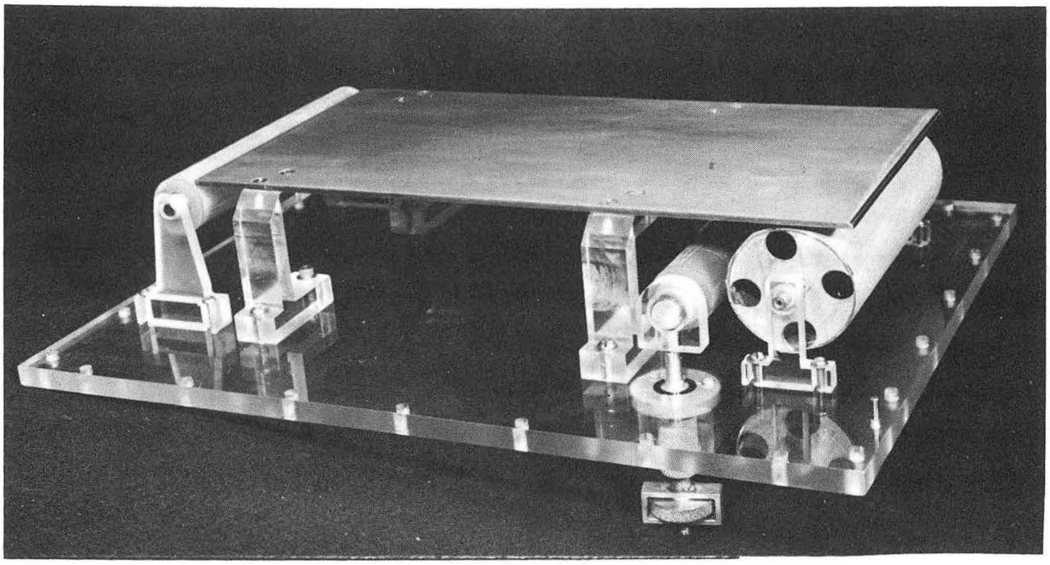

ZN-5041

Fig. A9-a

expended on constructional details of this nature.

d. Belts

Requirements for the wall-belt material include the following: 1) high tensile strength, 2) low elasticity, 3) good wear-resistance, 4) resistance to electrolytic solutes which may be added to the water, and 5) either be available as continuous belts or be relatively easy to splice. In addition to these, it is desirable to have a very thin, flexible material. It was finally decided that mylar film provided a good approximation to the above properties. After considerable testing, a film thickness of .002 inches was chosen. Splicing of the belt onto the wall-unit also turned out to be a difficult task, for any irregularities in the splice result in either wrinkles or drifting or both. Furthermore, if the splice is made perpendicular to the length of the belt, it causes an abrupt change in rigidity at the splice, resulting in catching and slipping on the edges of the wall. To prevent this, the splice is made at approximately a 45° angle. Since many tests have showed that splicing of the belts is very critical to good operation, I have included in the appendix a technique which I have found to be fairly satisfactory.

A further problem associated with the belts is providing good friction on the drive roller. Natural rubber is fine when dry but slips considerably when wet. Similarly, it was found that a stainless steel roller did not provide sufficient friction. The final unit consists of a stainless steel drive roller coated evenly with R.T.V.-102 self-curing silicone rubber. This provides excellent friction with mylar both dry and wet.

The phenomenon which I call "drifting" of the wall-belts requires some further clarification. It is the tendency of the belts, while running, to move slowly to one side or the other on the rollers. This problem is always encountered in situations where continuous conveyor belts are used. It is caused by the tendency of the belts to move toward the region of highest tension, and is normally solved by "crowning" the drive rollers (making them thicker in the center than at the ends). This forces the belt to drift toward the center. Crowning of the rollers in this equipment, however, produces excessive and unwanted wrinkles in the mylar belts. The only recourse is to maintain control by independent tension adjustment at both ends of the tension roller. This method required considerable practice, but has been found to be adequate to maintain good operation for periods of up to about half an hour.

2. Remaining Tunnel Sections

The test section is constructed entirely of Lucite to permit ease of fabrication and good visibility of the experiment. The test section is shown in Fig. A-10. Three ports were provided on each side so that objects for study or measuring devices may be readily mounted inside. Each port plug is sealed with an O-Ring and fastened with four screws to the test section wall. These plugs may be easily modified to serve a variety of mounting purposes.

The flow-straightening section is also constructed of Lucite and has one port on each side for flow measurements. It is designed so that honeycomb, screens or other flow-straightening equipment can be inserted.

The converging and diverging sections, shown in Fig. A-11, are made of 1/16 inch welded sheet stainless steel and have square cross-sections throughout.

It was anticipated that the presence of the converging and diverging sections might necessitate the introduction of some additional lengths of plain, smooth tunnel to allow further development of the velocity profile or to prevent propagation of the effects of the converging section back into the test section. These "calming sections" may be easily constructed of Lucite or sheet metal and flanged into place were needed.

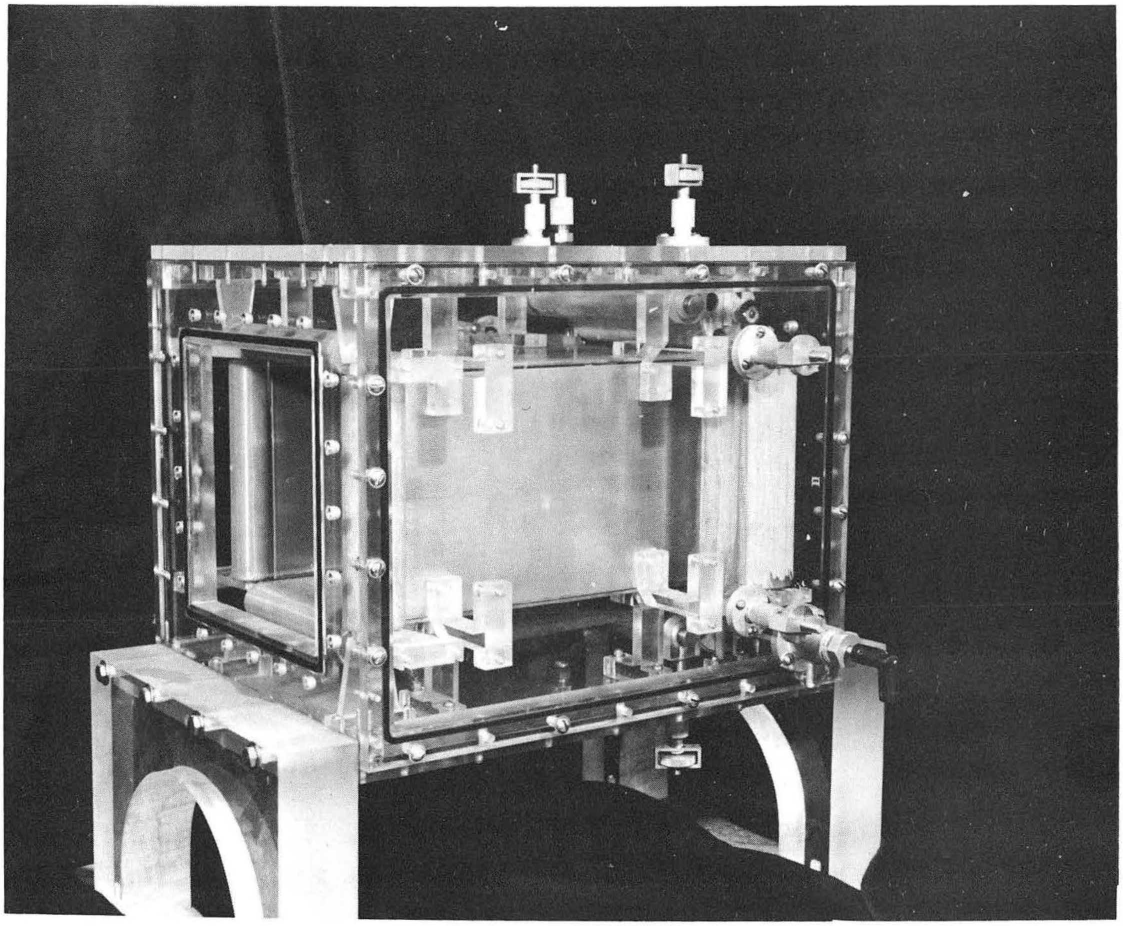

ZN-5042

Fig. A-10

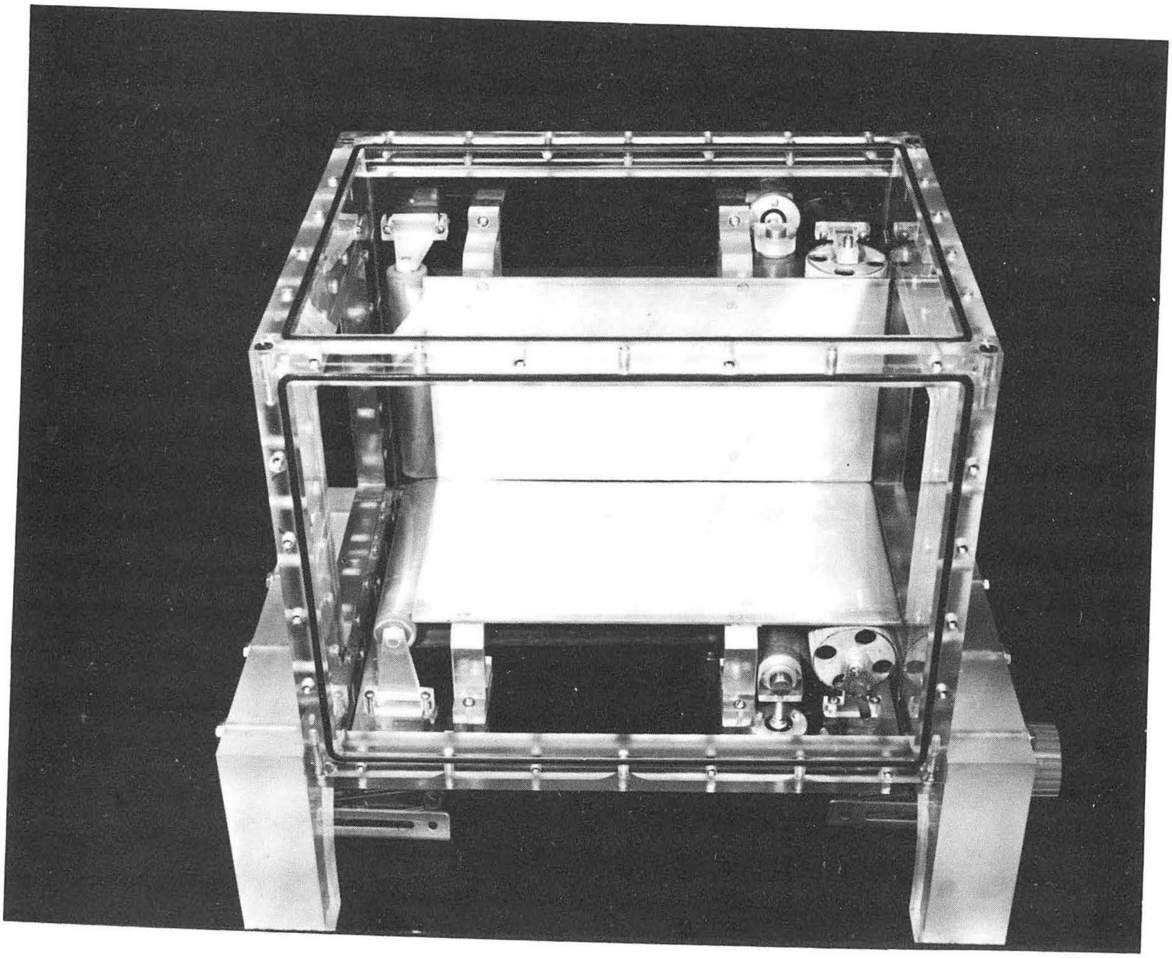

ZN-5043

Fig. A10a.

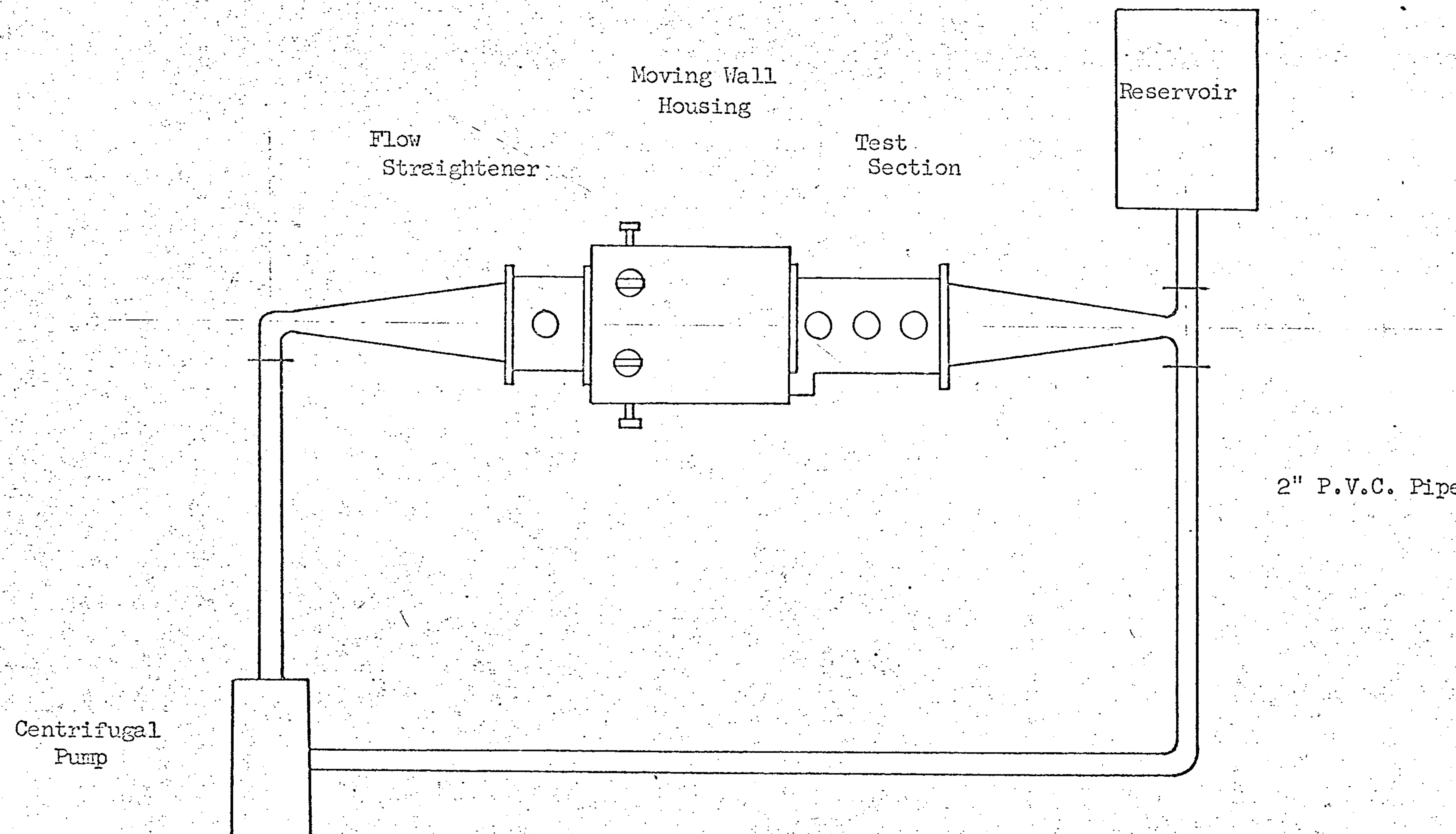
Moving Wall
Housing
Flow
Straightener
Test
Section
Reservoir
2" P.V.C. Pipe
Centrifugal
Pump

FIGURE A-11

3. Recycle System

Water is recirculated from the exit of the converging section to the entrance of the diverging section through a system consisting of nominal 2-inch schedule 40 polyvinylchloride (PVC) pipe and a standard centrifugal pump. The overall system is shown in Fig. A-12. A reservoir is provided as shown to keep the apparatus full and at a constant head, and to facilitate filling.

Pumping is done by a standard centrifugal pump whose maximum capacity is approximately 50 gallons per minute. Primary regulation of the rate of flow is performed by speed control of the pump, while a needle valve in a small bypass is used as a trimming device. The pump operates well at low speeds because the system is closed, providing a flooded suction, and the pumping head is reduced to zero with the flow rate.

Pressure drops in the pipe were calculated using a Fanning friction factor.

For the square tunnel sections, the same relation is used with the pipe radius replaced by twice the mean hydraulic radius defined as:

$$R_h = \frac{S}{Z}$$

where S = cross-sectional area

A = wetted perimeter

Head losses in the diverging and converging sections were based on the equations

$$h = \frac{K(V_1 - V_2)^2}{2g_c}$$

$$K = 0.0110\ \alpha^{1.22}$$

where h = head loss

V_1 = upstream velocity

V_2 = downstream velocity

K = correction factor

α = angle of divergence in degrees

g_c = 32.17 (ft.)(lb. mass)/(sec.^{2})(lb. force)

A summary of all head losses is given in Table I for the maximum expected flow rate of 30 gallons per minute.

Table I

PRESSURE DROPS

Item	Head Loss (Ft.)
12 feet of 2 inch pipe	0.35
4 inches of 1/16 inch honeycomb	0.01
Two 2 inch square standard radius 90° elbows	0.30
One 2 inch round sharp radius 90° elbow	0.20
Converging and diverging units	0.10
Total head loss	0.96 feet

It is seen that the total pressure drop in the system is quite low. The power required at the pump is correspondingly low. This is found from an overall mechanical energy balance, represented simply, for this case, by the total pressure drop times the total mass flow rate:

$$\text{Power} = \left(\frac{1 \text{ ft. lb}_f}{\text{lb}_m}\right) (30 \text{ g.p.m.}) \left(\frac{6 \text{ lb}_m}{\text{gal.}}\right)$$

$$= \left(\frac{180 \text{ ft. lb}_f}{\text{min}}\right).$$

This corresponds to only 0.0055 horsepower. Assuming, to be conservative, that the pump actually dissipates about one tenth of a horsepower, or 255 BTU per hour, to the water as heat, the temperature rise of the water should be approximately three degrees Fahrenheit per hour. This causes a 4-1/2 percent per hour decrease in the viscosity of the water. Since it is not anticipated that the apparatus will be run for more than about 15 minutes at a time, this temperature is not considered a problem.

B. A FLOW VISUALIZATION TECHNIQUE - THE TELLURIUM METHOD

A technique which has been developed recently for the visualization of aqueous flows is called the tellurium method. It has been found that when tellurium is used as a cathode in an electrolytic cell having an inert anode and an aqueous electrolyte, a black, dye-like substance is emitted from its surface. The dye-like substance is actually a colloidal suspension of tellurium particles. The applied potential difference for emission is typically 1-10 volts. Wortmann[6] was the first to describe the technique of using tellurium cathodes for flow visualization. The particles of tellurium in the suspension diffuse and settle very slowly in water, making them especially useful for tracing streamlines of flow. The probable mechanism[7] for formation of the tellurium suspension involves two steps: first, formation of the doubly charged tellurium ion $Te^{=}$ on the electrode surface, and second, a charge transfer reaction in which a molecule of dissolved oxygen picks up two electrons from a tellurium ion. The first step may involve either direct pickup of two electrons by a tellurium atom to form $Te^{=}$ or pickup of one electron to form Te^{-} followed by a disproportionation reaction. Namely:

1. a) $$Te + 2e^{-} \rightarrow 2Te^{=} \qquad \text{(B-1)}$$

   b) $$Te + e^{-} \rightarrow Te^{-} \qquad \text{(B-2)}$$

   $$2Te^{-} \rightarrow Te + Te^{=}$$

It is thought that the latter accounts for about 75% of $Te^{=}$ formed; the former, 25%. The second step occurs in the bulk solution:

2. $$2Te^{=} + O_2 \rightarrow 2Te + 2O^{=} \qquad \text{(B-3)}$$

The flow visualization technique described by Wortmann involves the placing of a thin tellurium wire crosswise to the flow. He then periodically applies a pulse of potential, causing a line, or long thin cloud, of tellurium to leave the wire surface and travel downstream with the local fluid velocity. In this way he has, for instance, visualized the flow in a boundary layer.

The use of tellurium wires represents one of the several ways of applying the method to flow visualization. Another method is to place small "spots" of tellurium along the length of a wire of inert metal. This wire is then placed crosswise to the flow as before and a steady potential applied. The result is a series of continuous streaks flowing downstream with the fluid, much the same as smoke in a wind tunnel.

A third method of using tellurium for flow visualization involves the use of tellurium "probes". Eichorn[8] has described a technique whereby tellurium is melted in a soft glass tube, which is then drawn into a short capillary. The capillary is cut in the center, leaving two probes such as shown in Fig. B-1. The probe is placed in an aqueous solution as the cathode of an electrolytic cell. The potential may then be applied continuously or in pulses to give black streaks eminating from the tip of the probe. Eichorn used this method to study natural convection.

It is proposed that appropriate variations of the tellurium method be used for flow visualization in the water tunnel. Tellurium wires would be used for visualizing velocity profiles in mainstream or boundary layer regions, whereas the probes would be useful to pinpoint local flow conditions where it is desired to follow a particular streamline. An example of the use of probes is given in the next section.

The switching procedure used to obtain intermittent streaks of

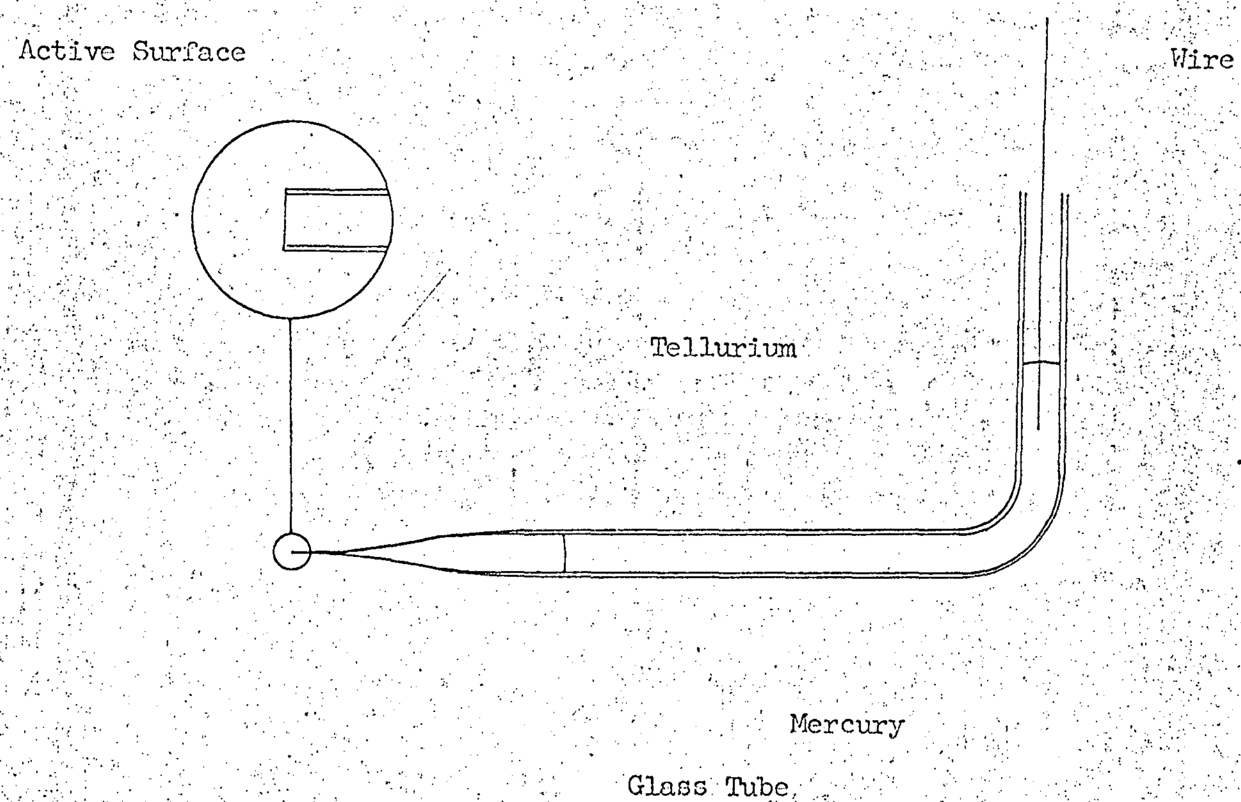

FIGURE B-1

tellurium would be accomplished by using an impulse generator made up of a multivibrator and two univibrators. The multivibrator would trigger the two univibrators every t_2 seconds. One univibrator would respond with a pulse of current to the tellurium lasting a time t_1 seconds ($t_1 < t_2$); while the other univibrator would activate a pulse camera to take a photograph. In this way, accurate records of the fluid flow may be obtained.

C. A TYPICAL EXPERIMENT - SEPARATED FLOW IN A RECTANGULAR NOTCH

The study of eddies formed as a result of steady, separated flows is not a simple matter because such situations are normally not stable and must be examined in a transient condition. One possibility of examining such flows in the steady state exists in the case of flow past a rectangular cavity, or notch, in the wall of a channel (See Fig. C-1).

It has been shown[9] that for such a case a stable eddy does exist, provided the dimensions of the "notch" are within certain limits. Direct measurement of fluid velocities throughout such a notch, however, have not been found in the literature. It is felt that an experiment resulting in such velocity measurements would contribute materially to the understanding of separated flows.

Moffatt[10] has demonstrated theoretically the existence of a series of eddies, diminishing rapidly in size and intensity, in a corner with fluid flowing past it; for a 90° corner, he predicts a diminishing of intensity between adjacent eddies by a factor of about 2000. Such "secondary" eddies have been observed in a rectangular notch[11] but it would be desirable to make velocity measurements as well.

The water tunnel described in this paper is well suited to the adaptation of such an experiment. For this reason, a rectangular notch, one inch square by six inches long, has been incorporated in the upstream end of the test section, as illustrated in Fig. C-2.

As shown in Fig. C-2, the upstream side of the notch is formed by a part of the moving wall housing, while the bottom and downstream sides are built into the test section. This was done to keep the notch as close as possible to the end of the moving walls, thereby insuring

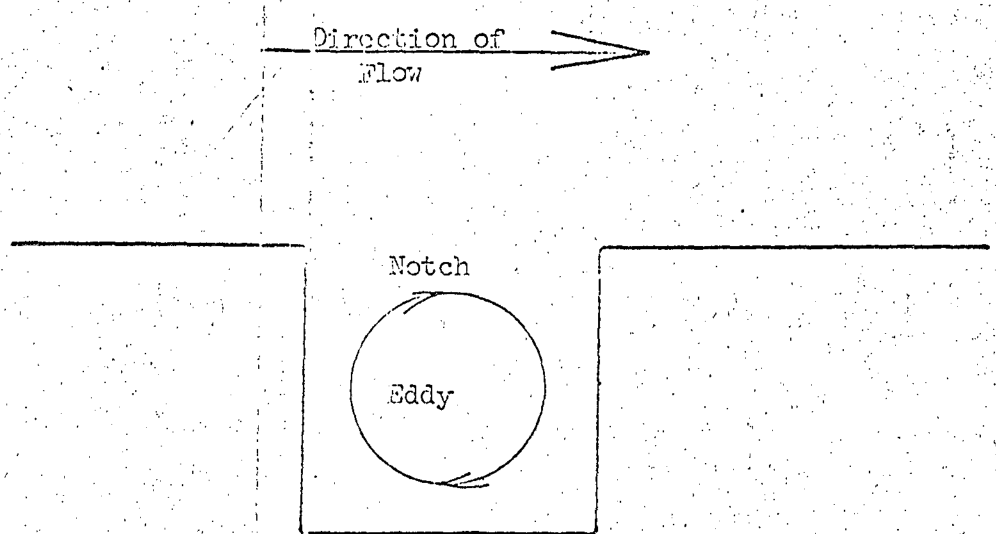

FIGURE C-1

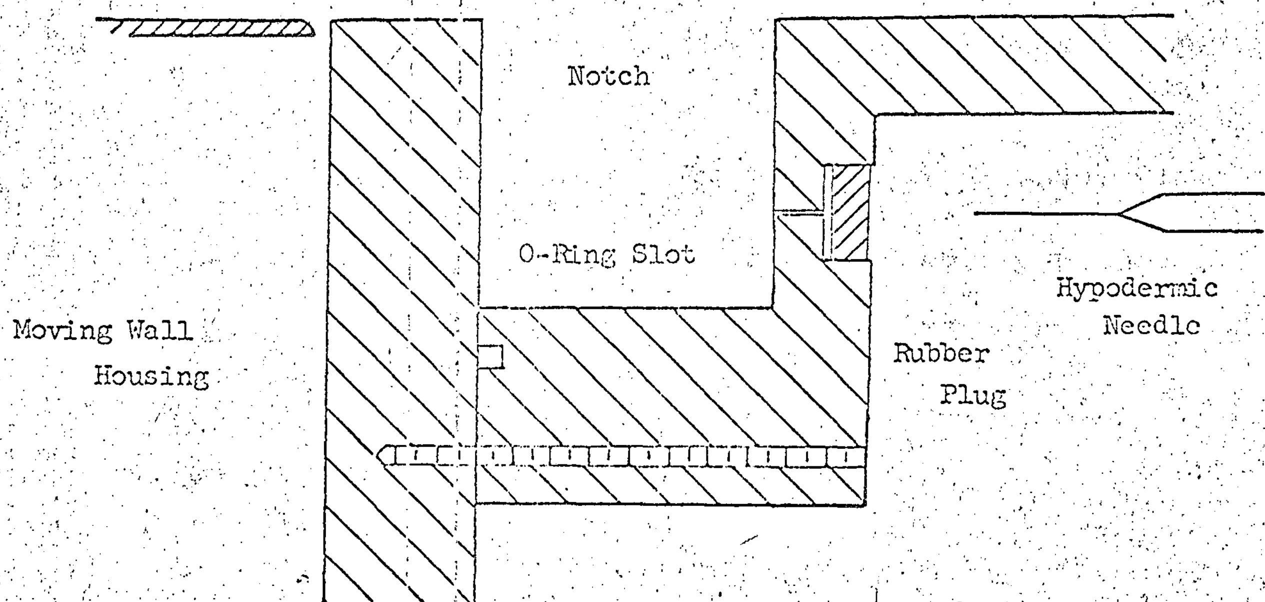
Notch
O-Ring Slot
Moving Wall
Housing
Rubber
Plug
Hypodermic
Needle

FIGURE C-2

the minimum boundary layer growth prior to the notch. The thickness of the housing wall is 3/4 inch and this is the distance over which the boundary-layer will grow prior to the notch. The expected boundary layer thickness at the entrance to the notch may be seen from Fig. A-4 for various Reynolds numbers by looking at the point 3/4 inch downstream of the beginning of the boundary layer.

1. Flow Measurements in the Notch

Visualization of the flow in the notch may be accomplished by the introduction of some visible particles into the water. Photographs may then be taken from the end of the notch. It is felt that a modification of the tellurium method may be used to obtain velocity measurements in the notch.

The procedure would be to insert a very thin tellurium probe, similar to Eichorn's, into the notch at any desired position. Then provide a pulsed current to the probe by an impulse generator such as used by Wortmann, while simultaneuously triggering a pulse-type camera. Thus, photographs would be obtained at precisely known intervals, and velocity measurements made by measuring the distance travelled by tellurium traces between photographs.

The probes themselves would be made by filling thin hypodermic needles with tellurium. The use of glass capillary probes would be inconvenient because of their lack of strength. The hypodermic needle probes, moreover, can be inserted into the notch through a self-sealing rubber plug in the notch wall, as illustrated in Fig. C-2. This method allows easy removal of the probes when desired.

Tellurium probes made of hypodermic needles have been constructed and subjected to exploratory tests as a part of this investigation. The probes were made by filling the upper, cupped section of the hypodermic needles with shavings of tellurium and then melting the Te in a muffle furnace. Since tellurium oxidizes readily when heated, a nitrogen atmosphere was provided.

It was found in tests with these probes that a potential of 1 volt was not sufficient to produce a significant dye trace in ordinary tap water. A 6 to 10 volt potential produced a better trace but is not practical because of hydrogen evolution on the needle itself. A thin insulating coating of plastic on the needle should prevent hydrogen evolution, but further testing in this area is needed. It was found, however, that addition of small amounts of electrolyte, such as common salt, to the water was sufficient to allow very good tellurium traces in the 1 volt range. The presence of such electrolytes in the water tunnel should not present any significant problems.

The multivibrator required to provide appropriately spaced tellurium traces for measurements at all flow conditions should operate at a time between pulses, t_2, of from 40 msec to 3 sec, while the univibrator used to provide current to the probe should provide pulse times t_1 of 2 msec to 150 msec.

SUMMARY

A recirculating water tunnel has been developed to provide low-turbulence flow at Reynolds numbers up to about ten thousand with a flat velocity profile. The moving-wall method has been used to accomplish these conditions. Operation of the moving-wall mechanism is largely a matter of technique, and it should be possible to operate it for periods exceeding 30 minutes with no modification of the system. One of the main problems initially associated with the moving-wall system, that of leakage, has been solved by enclosing the entire system in a housing filled with water.

An attempt was made to obtain a theoretical basis for designing the length of the moving walls. This attempt was based on the assumption that the flow does not resemble isotropic turbulence in the wake of the flow straightener. The validity of this assumption, however, cannot be determined until the tunnel is tested under operating conditions.

One of the problems remaining is the drifting of the belts. Successful elimination of this problem is again largely a matter of technique. Some of the most important design parameters and specifications of the system are listed below:

<u>Performance</u>

Maximum tunnel Reynolds number (Re_t) = 15,000

Maximum bulk average water velocity = 10 cm/sec

Maximum volumetric flow rate = 30 gal/min

Tunnel

Shape: Square cross-section

Flow area: 36 square inches

Material: Stainless steel and plexiglas

Moving Walls

Belt material: Mylar

Thickness of belts: .002 inches

Width of belts: 5-7/8 inches

Drive System

Diameter of drive rollers: 2 inches

Diameter of idler rollers: 1 inch

Surface of drive rollers: RTV-102 silicone rubber

Surface of idler rollers: Natural rubber

Bearings: Nylon-sleeve

Gears: Brass, 45° bevel

Torque required to drive the complete mechanism (wet, with belts): 1 ft-lb.

Miscellaneous

Return-flow pipe: nominal 2-inch schedule 40 p.v.c.

Length of moving wall section: 14-1/2 inch

Length of flow-straightening section: 7 inch

Length of test-section: 12 inch

Length of converging and diverging sections: 23 inches each

Total number of tapped holes: 388

ACKNOWLEDGMENTS

The author would like to thank Professor J. S. Newman for his inspiration and advice throught this work. Special thanks are also due to Mr. D. N. Voronin for his invaluable advice and diligence in the construction of the equipment.

This work was done under the auspices of the United States Atomic Energy Commission.

Appendix A

Laminar Decay Behind a Flow Straightener

The x-component of the Navier-Stokes momentum equation is:

$$\rho\left(U\frac{\partial u}{\partial x}+V\frac{\partial u}{\partial y}\right)=-\frac{\partial p}{\partial x}+\mu\left(\frac{\partial^2 u}{\partial x^2}+\frac{\partial^2 u}{\partial y^2}\right)$$

Assuming $\frac{\partial p}{\partial x}$ small and

$$u = U + u'$$

where $u' \ll U$

the above equation may be linearized. Neglecting quadratic terms in u' and noting from the continuity equation that the component of velocity in the y-direction, V, must be of the same order as u', the momentum equation becomes:

$$\rho\, U\frac{\partial u'}{\partial x}=\mu\left(\frac{\partial^2 u'}{\partial x^2}+\frac{\partial^2 u'}{\partial y^2}\right)$$

Or, using the non-dimensional variables introduced in the text:

$$\frac{\partial u'^*}{\partial x^*}=\frac{1}{Re_h}\left(\frac{\partial^2 u'^*}{\partial x^{*2}}+\frac{\partial^2 u'^*}{\partial y^{*2}}\right)$$

The boundary conditions are:

1) $u'^* = \frac{A}{U}\cos 2\pi y^*$ at $x^* = 0$

2) $\frac{\partial u'^*}{\partial y^*} = 0$ at $y^* = \frac{n}{2}$ $(n = 0, 1, 2 \ldots)$

3) $u'^* \neq \infty$ at $x = \infty$

Solve by separation of variables:

assume $u'^* = X(x^*)\cdot Y(y^*)$

therefore $X'Y = \frac{1}{Re_h}(YX'' + XY'')$

or $\frac{Y''}{Y} = \frac{Re_h X' - X''}{X}$

Letting each side equal $-K^2$,

$$Y'' + K^2 Y = 0$$

therefore $Y = A \sin Ky^* + B \cos Ky^*$

A must be zero since u'^* is an even function of y (B.C.1).

Therefore $Y = B \cos Ky^*$

also $X'' - Re_h X' + K^2 X = 0$

therefore $X = c_1 e^{-r_1 x^*} + c_2 e^{-r_2 x^*}$

but c_1 must be zero from B.C. 3.

Thus $X = ce^{-rx^*}$

where $r = -Re_h \sqrt{Re_h^2 + K^2}$

Therefore:

$$u'^* = B \cos Ky^* \, e^{-rx^*}$$

but B = A from B.C.1. Using B.C.2:

$$\frac{u'^*}{y^*} = - CK \sin Ky^*$$

therefore $\sin K \frac{n}{2} = n\pi$

$$K = 2n\pi$$

Therefore, the final solution becomes:

$$u'^* = \frac{A}{U} \cos 2\pi y^* \exp -rx^*$$

where $r = -Re_h + \sqrt{Re_h^2 + 4\pi^2}$.

Appendix B

A Technique for Splicing of the Belts

Splicing of the belts has been found to be a very critical procedure. It must be done evenly and with no tension to prevent wrinkling and drifting of the belts. The technique described here has been found to be satisfactory and may be helpful to future operators.

1. Place a complete wall-unit on a workbench with the stainless steel wall facing up. Cut a piece of .002 inch thick mylar to the proper width (about 5-7/8 inches) and 4 or 5 inches longer than required.
2. Thread the mylar belt through the rollers on the wall-unit, overlapping it on the stainless wall (4 or 5 inches should overlap). Align both ends of the belt carefully.
3. Wet the stainless wall and overlapping areas of the mylar with denatured alcohol. This serves to adhere and hold the belt in place.
4. With a metal straight-edge razor blade, cut through the overlapping part of the mylar at about a 45° angle. Remove the two triangular pieces which have been cut. Realign the belt and add alcohol along the cut if necessary. The belt should no longer overlap, but should be butted together at a 45° angle and be ready for splicing.
5. Prepare the splicing tape as follows: lay a 16" strip of 1/2" wide, .001" thick pressure-sensitive mylar tape sticky side up lengthwise on a one foot metal ruler. Wrap the tape around the ends of the ruler and secure the ends of the tape into place on the back of the ruler with masking tape. Allow the alcohol on the surface of the belt to evaporate. The alcohol beneath the belt will not evaporate, but will hold the belt firmly in place for splicing.
6. Align the tape and ruler with the cut in the mylar and press gently into place, completing the splice.

7. Remove the ruler and trim the tape to the edges of the belt.

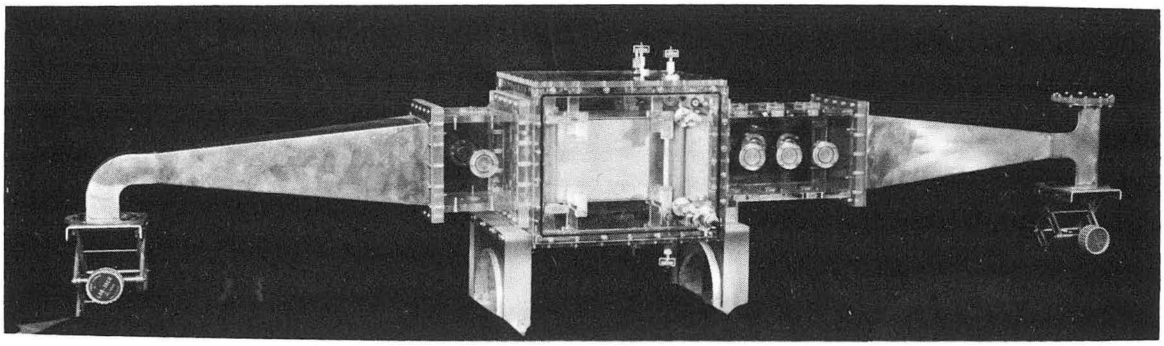

ZN-5044

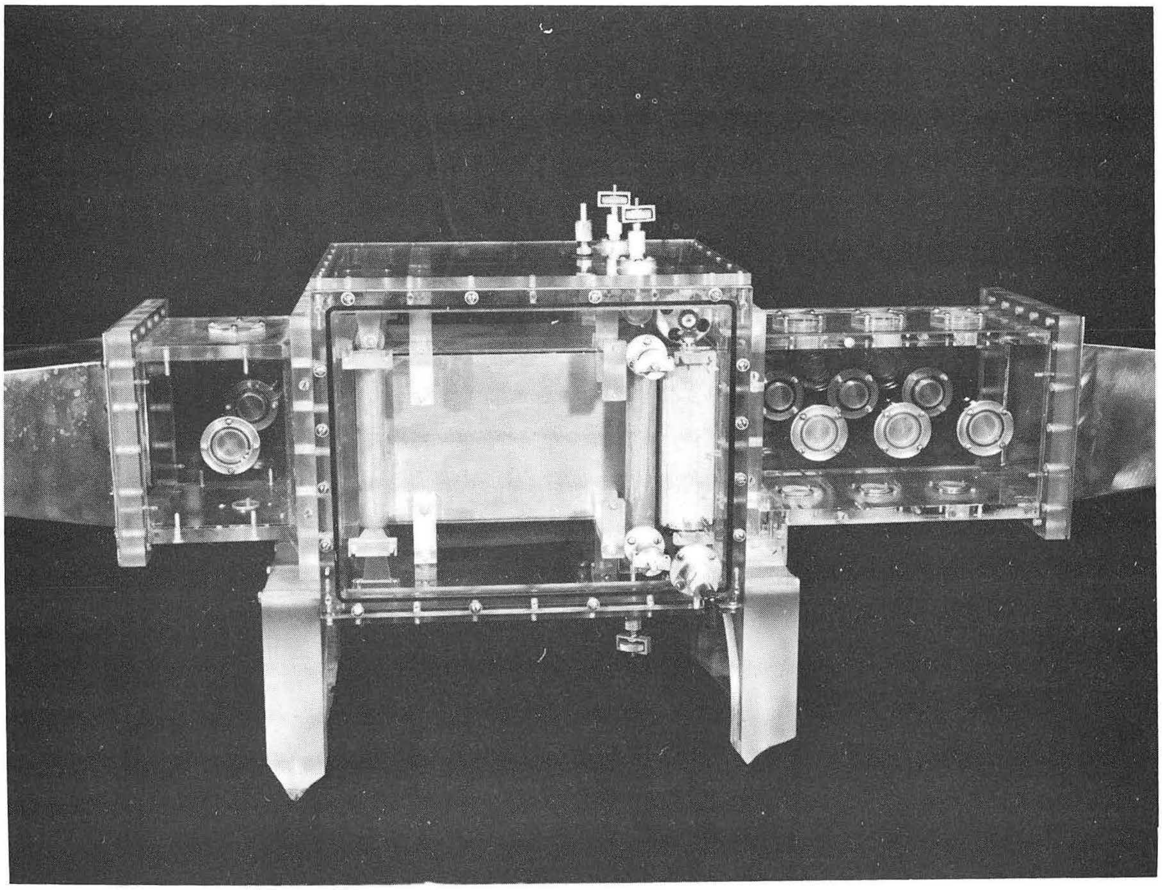

ZN-5045

REFERENCES

1. H. Schlichting, Boundary Layer Theory, McGraw-Hill Publishing Company, New York (1960) p. 163.
2. ibid, p. 171.
3. ibid, p. 470.
4. G. I. Taylor, "Statistical Theory of Turbulence", Proc. Roy. Soc. London, A151, 421-478 (1935).
5. G. K. Batchelor, The Theory of Homogeneous Turbulence, Cambridge University Press, (1953).
6. F. X. Wortman, "Eine Methode zur Beobachtung und Messung von Wasserstomungen mit Tellur", Zeit. f. ange. Physik, 5, 201 (1953).
7. ibid, p. 202.
8. R. Eichorn, "Flow Visualization and Velocity Measurement in Natural Convection with the Tellurium Dye Method", J. Heat Transfer, 1961, p. 379.
9. A. Roshko, "Some Measurements of Flow in a Rectangular Cutout", NACA TN 3488, 1955.
10. H. K. Moffatt, "Viscous and Resistive Eddies Near a Sharp Corner", J. Fluid Mech. 18, 1 (1964) p. 1.
11. K. Wieghardt, "Erhohung des turbulenten Reibungswiderstandes durch Oberflachenstorungen", Forschungsbericht, 1563, ZWB, March 19, 1942.